Coupling of InGaN quantum-well photoluminescence to silver surface plasmons

I. Gontijo, M. Boroditsky, and E. Yablonovitch
UCLA Electrical Engineering Department, University of California, Los Angeles, California 90095

S. Keller, U. K. Mishra, and S. P. DenBaars
Materials Science and Electrical Engineering Departments, University of California, Santa Barbara, California 93106-5050

(Received 10 May 1999)

The coincidence in excitation energy between surface plasmons on silver and the GaN band gap is exploited to couple the semiconductor spontaneous emission into the metal surface plasmons. A 3-nm InGaN/GaN quantum well (QW) is positioned 12 nm from an 8-nm silver layer, well within the surface plasmon fringing field depth. A spectrally sharp photoluminescence dip, by a factor ≈55, indicates that electron-hole energy is being rapidly transferred to plasmon excitation, due to the spatial overlap between the semiconductor QW and the surface plasmon electric field. Thus, spontaneous emission into surface plasmons is ≈55 times faster than normal spontaneous emission from InGaN quantum wells. If efficient antenna structures can be incorporated into the metal film, there could be a corresponding increase in external light emission efficiency.
[S0163-1829(99)08939-0]

Metals support collective oscillations of the conduction electrons, called bulk plasmons, at the plasma frequency ω_p. Surface plasmons of a lower frequency ω_{sp} can also be excited by high energy electron beams or by light. Pioneering studies[1,2] have shown that the fluorescence lifetime of molecules can be affected by a metal surface placed in close proximity. Since then, there has been much progress in coupling surface plasmons (SP's) to different radiative systems. The optical transmission of thick metal films perforated with a periodic array of subwavelength holes[3] is enhanced by plasmon coupling from the front to the back surface. Light absorption enhancement in thin silicon films by metal islands was shown by Stuart and Hall.[4] Spontaneous emission enhancement from a quantum well under a metal grating was observed by Hecker *et al.*,[5] but was probably due to enhanced pump absorption, as in the Stuart and Hall case.[4] In Hecker's case, the quantum well was too distant from the silver to significantly increase the spontaneous emission rate itself. Barnes *et al.*[6] did see a modification of spontaneous emission from Eu ions into surface plasmons, particularly when placed very near the silver surface. In that case, the spontaneous emission spectral line was far removed from the surface-plasmon frequency. Indeed there has been a long record of studies of the spontaneous emission from atoms and molecules near silver surfaces. We report the first example of resonant coupling of semiconductor spontaneous emission into surface plasmons, for which $E_{gap}=\hbar\omega_{sp}$, where E_{gap} is the semiconductor band gap. At the end of this paper, we will show that the photophysics of a semiconductor radiator is inherently different from the photophysics of a molecule above a silver surface, since the semiconductor case is immune to a particular nonradiative excitation process in the metal.

In silver[7,8] the bulk plasmon energy is $\hbar\omega_p=3.76\,\mathrm{eV}$ and the surface-plasmon energy is somewhat lower, below 3 eV, depending on the refractive index of the adjacent dielectric. This energy range is fortunate since the new wide-band-gap nitride semiconductors can be resonant with surface plasmons on Ag. GaN/InGaN quantum wells have the right photoluminescence emission energy to excite surface plasmons at the semiconductor-metal interface.

The surface-plasmon frequency condition is given by $\varepsilon'_{Ag}(\omega)+\varepsilon'_{GaN}(\omega)=0$, where and ε'_{Ag} and ε'_{GaN} are the real parts of the dielectric constants of Ag and GaN, respectively. Thus the GaN dielectric constant pulls the Ag surface-plasmon energy down to $\hbar\omega_{sp}=2.92\,\mathrm{eV}$. If the GaN quantum well is spaced close to the Ag-GaN interface, a strong quantum electrodynamical coupling between the quantum-well (QW) and the SP can take place, with an electron hole pair in the semiconductor spontaneously recombining and producing a surface plasmon, instead of a free-space photon. The surface-plasmon fringing field penetration depth into the semiconductor is given by $z=\lambda/2\pi[(\varepsilon'_{GaN}-\varepsilon'_{Ag})/\varepsilon'^{2}_{GaN}]^{1/2}=40\,\mathrm{nm}$ for Ag on GaN at $\hbar\omega=2.92\,\mathrm{eV}$, where $\varepsilon'_{GaN}=-\varepsilon'_{Ag}\approx 6$.

An InGaN/GaN single quantum well (SQW) grown by metallo-organic chemical-vapor deposition was used in our experiments. The growth began on a sapphire substrate with a 1.5-μm GaN:Si (GaN, Si-doped) buffer layer, followed by 28 nm of $In_{0.04}Ga_{0.96}N$:Si which served as a reference layer, 6-nm GaN and then the 3-nm $In_{0.18}Ga_{0.82}N$ SQW. The epitaxy was completed with the deposition of a 12-nm-thick GaN:Si spacer layer. Therefore, the SQW is only 12 nm below the surface, which is well within the fringing field depth of the SP. Details on the growth conditions can be found elsewhere.[9]

An 8-nm layer of silver was deposited on only one-half of the sample surface by electron-beam evaporation. In this way, a direct comparison of the photoluminescence (PL) spectrum of the Ag-coated and the uncoated parts of the sample could be made. A continuous wave He-Cd laser operating at 326 nm and focused to 150 W/cm^2 was employed for PL excitation and the sample was kept at room temperature. PL was collected by a lens, dispersed by a monochromator and detected by a Si photodiode.

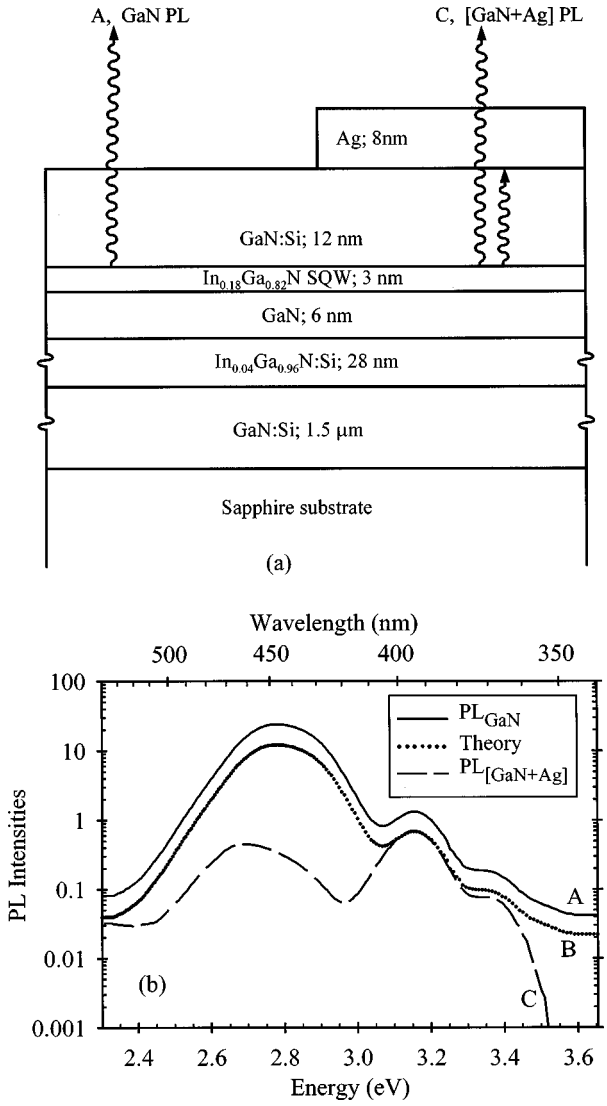

FIG. 1. Interaction of single quantum-well photoluminescence (PL) and surface plasmons in Ag. (a) shows the experimental geometry. In (b), curve *A* is the PL spectrum obtained from the uncoated semiconductor. Curve *B* is the PL from the uncoated semiconductor, corrected for the absorption attenuation that would have been caused by a Ag film of 8 nm thickness. Curve *C* is the actual PL spectrum observed above the 8 nm Ag film.

Figure 1(a) shows some details of the experiment. Curve *A*, in Fig. 1(b), is the PL spectrum measured on the uncoated part of the GaN sample. The SQW PL peak occurs at about 2.8 eV, with a second peak about 20× smaller, appearing at 3.17 eV, due to the reference layer. When photoluminescence is excited on the Ag-coated part of the sample, the transmission and reflection properties of the Ag layer have to be taken into account, for both the pump light, and the PL emission. If plasmon excitation is neglected, the transmission can be easily calculated, using the standard Fresnel theory[10] and the known values of the refractive index and extinction coefficient of silver. The product of the pump and PL transmission, $T_P \times T_{\mathrm{PL}}(\omega)$, is the overall absorption/reflection correction due to the Ag layer, which is modest, only ≈ 0.5. Thus, curve *B* is reduced by the $T_P \times T_{\mathrm{PL}}(\omega) \approx 0.5$ attenuation, from the measured PL on the uncoated sample, curve *A*.

When PL is excited and collected from the Ag-coated part of the sample however, a completely different picture emerges as shown by curve *C* in Fig. 1(b). At the cladding layer PL peak (3.17 eV), the experimental ''*C*'' and predicted ''*B*'' curves coincide, i.e., in this region, the usual absorption and reflection properties of the silver layer can indeed account for the PL decrease from curve *A*. On the other hand, around the 2.8-eV SQW emission, the external PL is reduced by almost two orders of magnitude. We interpret this as the result of spontaneous energy transfer from the SQW electron-hole pairs into the electromagnetic surface-plasmon modes of the silver layer. For energies above 3.4 eV, a very strong attenuation of the external PL is again seen, which is attributed to excitation of the bulk plasmon in silver. These external PL attenuation dips are more clearly seen in Fig. 2, which shows the ratio of external PL anticipated, curve *B*, divided by the external PL actually observed, curve *C*. The features of Fig. 2 include the surface-plasmon resonance centered at 2.9 eV with a full width at half maximum of 193 meV, corresponding to a *Q* of 15. In addition, between 3.4 and 3.6 eV there is a significant external PL dip, due to the tail of the bulk plasmon, which is centered at 3.76 eV in Ag.

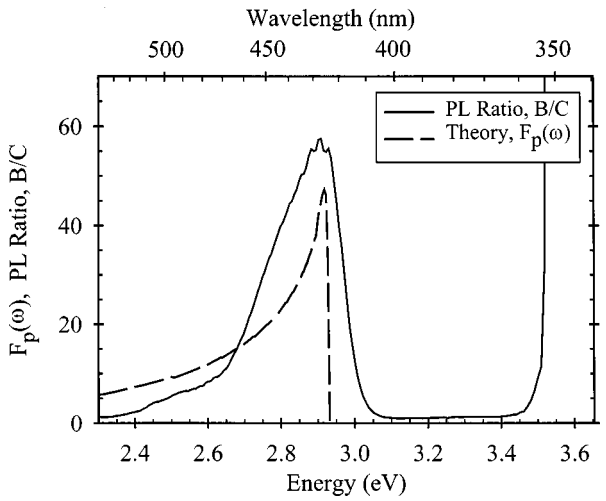

FIG. 2. Surface-plasmon-induced spectral luminescence dip, plotted as a positive quantity (solid curve), given by curve *B* divided by curve *C* from 1(b). We interpret this as a Purcell enhancement factor $F_p(\omega)$ for radiation into surface-plasmon modes rather than into external electromagnetic waves. The sharp rise near 3.5 eV is due to bulk plasmon excitation.

We must emphasize that the attenuation of external PL at frequencies corresponding to the surface and bulk plasmons is not caused by the absorption/reflection properties of the Ag film. Instead, it results from the competition between spontaneous emission into external electromagnetic modes versus spontaneous emission into plasmon modes. We have carefully calibrated the internal quantum efficiency of this InGaN SQW and we find it to be >90%. Thus, nonradiative processes hardly compete with the enhanced spontaneous emission into plasmons modes. In the uncoated part of the sample, both radiative and nonradiative recombination are present, described by the recombination rates $\Gamma_0(\omega)$ and $\Gamma_{\mathrm{nr}}(\omega)$. In the Ag-coated part, the change in external quantum efficiency is attributed to a new spontaneous emission channel into surface plasmons, which do not escape externally. The total recombination rate is then $\Gamma_0(\omega)+\Gamma_p(\omega)$

$+\Gamma_{nr}(\omega)$. Thus, the ratio of the PL spectra from the uncoated and Ag-coated parts of the sample is a direct measurement of the recombination rate enhancement. This ratio, which is an analog of the Purcell[16] factor F_p, can be expressed simply as

$$F_p(\omega)=\frac{\Gamma_p(\omega)+\Gamma_0(\omega)+\Gamma_{nr}(\omega)}{\Gamma_0(\omega)+\Gamma_{nr}(\omega)}\approx 1+\frac{\Gamma_p}{\Gamma_0}. \qquad (1)$$

Our absolute luminescence calibration results indicate that the nonradiative contribution was negligible in this excellent InGaN sample. Therefore, those terms containing Γ_{nr} were dropped from the right-hand side of Eq. (1).

The plasmon modes can be analyzed by obtaining the dispersion relations for a metal slab between two dielectrics. For the infinitely thick metal case, where the metal lies in the semi-infinite space $z>0$, with the dielectric below ($z<0$), Maxwell's equations can be readily solved and boundary conditions can be matched at the interface, leading to

$$\varepsilon_1\gamma_2+\varepsilon_2\gamma_1=0, \text{ with } \gamma_i^2=k^2-\varepsilon_i\omega^2/c^2, \qquad (2)$$

where ε_1 and ε_2 are the dielectric functions of the dielectric and metal respectively, k is the wave vector, and ω the frequency. Combining these equations and solving for k, the dispersion relation for the surface plasmons is obtained:

$$k^2=\frac{\varepsilon_1\varepsilon_2}{\varepsilon_1+\varepsilon_2}\frac{\omega^2}{c^2}. \qquad (3)$$

If the metal does not fill the whole semi-infinite space $z>0$, but is of thickness t instead, then SP can be excited on both the top and bottom interfaces. For sufficiently small t, the SP's at both interfaces couple together, generating symmetric and anti-symmetric plasma oscillations.[11] Considering a metal slab of thickness t and dielectric constant ε_2 sandwiched between two dielectric media with constants ε_1 and ε_3, the boundary conditions lead to a dispersion relation of the form

$$(\varepsilon_1\gamma_2+\varepsilon_2\gamma_1)(\varepsilon_2\gamma_3+\varepsilon_3\gamma_2)-(\varepsilon_3\gamma_2-\varepsilon_2\gamma_3)(\varepsilon_1\gamma_2-\varepsilon_2\gamma_1)e^{-2\gamma_2 t}=0. \qquad (4)$$

It is clear that if the metal slab is very thick, the second term of Eq. (4) vanishes and one recovers the dispersion relations for the two uncoupled surfaces, given by the first term and Eq. (2). For smaller t, a complex situation ensues in which the plasmon of one interface is coupled to the plasmon of the other and their energies depend on the thickness t.

In the general case Eq. (4) is readily solved numerically, by treating its left-hand side as a function $f(\omega,k)$ of ω and k. The dielectric constants of silver and GaN used in the calculation were interpolated from tabulated[12,13] values. When Eq. (4) was solved for our experimental situation of a Ag layer 8-nm-thick deposited on GaN, the plot in the left-hand side of Fig. 3 was obtained. The two curves represent the normal or antisymmetric plasmon *A*, and the tangential or symmetric plasmon modes *S*. The words tangential and normal refer to the dominant direction of current flow in the Ag film. Note that for large wave vectors, the symmetric modes asymptotically approach an energy around 2.9 eV, which agrees closely with the spectral position of the plasmon dip in Fig. 2. In addition, it should be noted that the portion of the antisymmetrical plasmon branch between the c and c/n light lines must have a complex wave vector. These are ''leaky'' plasmon modes, which are not confined to the interface, but can propagate into the GaN, due to the small wave vector to the left of the c/n light line.

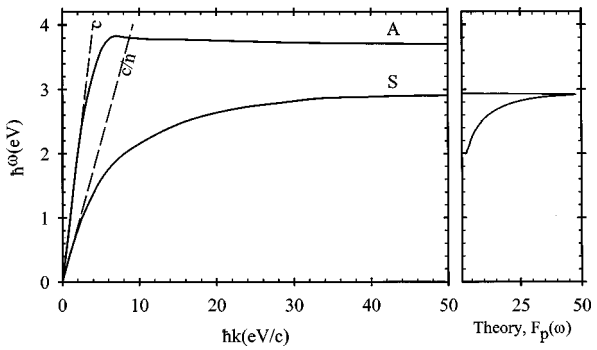

FIG. 3. Dispersion relations for an 8-nm Ag layer on GaN showing *A* the normal/antisymmetric and *S* the tangential/symmetric branches. The modes between the c and c/n light lines leak into the semiconductor. The plot on the right shows the calculated spectral shape (Purcell enhancement factor) for spontaneous emission into the tangential/symmetric mode. That mode simply consists of ac currents flowing tangentially in the Ag film, whose fringing fields extend into the SQW.

The local electric field of the plasmon mode at the SQW, $\mathbf{E}(a)$ can be used to estimate the recombination rate $\Gamma_p(\omega)$ of the SQW spontaneous emission into the plasmon continuum, by using Fermi's golden rule:

$$\Gamma_p(\omega)=\frac{2\pi}{\hbar}\langle\mathbf{d}\cdot\mathbf{E}(a)\rangle^2\rho(\hbar\omega), \qquad (5)$$

where $\mathbf{d}$ denotes the electron-hole pair dipole moment, a is the location of the SQW relative to the metal-semiconductor interface, and $\rho(\hbar\omega)$ is the mode density of plasmons. $\mathbf{E}(a)$ is normalized to a half quantum for zero-point fluctuations by the following denominator:

$$E^2(a)=\frac{\hbar\omega/2}{\frac{L^2}{4\pi}\int_{-\infty}^{\infty}[\partial(\omega\varepsilon)/\partial\omega]E_0^2(z)dz}E_0^2(a), \qquad (6)$$

where $\mathbf{E_0}(z)$ is the unnormalized plasmon electric field and L^2 is the in-plane quantization area. For a nondispersive medium, the integrand in Eq. (6) would be simply $\varepsilon E_0^2(z)$. In the present case, the medium is highly dispersive and the appropriate expression[14] to be used for the electric energy density is $[\partial(\omega\varepsilon)/\partial\omega]E^2/8\pi$. Note that $\varepsilon=\varepsilon(\omega,z)$ varies in frequency and also with the vertical position in the air/Ag/GaN structure.

The plasmon density of states is obtained in a manner analogous to other density of states calculations in solid-state physics. For a given frequency range $d\omega$, the number of corresponding modes in the two-dimensional k space is

$$\rho(\hbar\omega)=\frac{2\pi k\,dk}{(2\pi)^2 d(\hbar\omega)}L^2=\frac{L^2}{4\pi}\frac{d(k^2)}{d(\hbar\omega)}. \qquad (7)$$

Therefore, the density of plasmon modes $\rho(\hbar\omega)$ can be obtained from the derivative $d(k^2)/d\omega$ of the dispersion diagram $\omega(k)$ in Fig. 3. The density of states $\rho(\hbar\omega)$ and the

normalization in Eq. (6) can be combined with Eq. (5), to give the recombination rate into the plasmon modes

$$\Gamma_p(\omega)=\frac{2\pi d^2\omega E_0^2(a)}{3\hbar\int_{-\infty}^{\infty}[\partial(\omega\varepsilon)/\partial\omega]E_0^2(z)dz}\frac{d(k^2)}{d(\hbar\omega)}, \quad (8)$$

where the factor 1/3 comes from polarization averaging. This plasmon recombination rate has to be compared to the spontaneous emission rate $\Gamma_0(\omega)$ in bulk semiconductors, which can be calculated using the classical formula[15]

$$\Gamma_0(\omega)=\frac{4nd^2\omega^3}{3\hbar c^3}. \quad (9)$$

Combining Eqs. (1), (8), and (9), we obtain the Purcell enhancement factor[16] F_p for the spontaneous emission into the surface-plasmon modes:

$$F_p(\omega)=1+\frac{\pi c^3E_0^2(a)}{2\omega^2\int_{-\infty}^{\infty}[\partial(\omega\varepsilon)/\partial\omega]E_0^2(z)dz}\frac{d(k^2)}{d\omega} \quad (10)$$

The calculated $F_p(\omega)$ is shown both in Fig. 2 and on the right side of Fig. 3. Having dropped the nonradiative recombination terms from Eq. (1), there are no adjustable parameters in Eq. (10). Fairly good agreement is obtained between the experimental and calculated spectral shapes in Fig. 2. In particular, both are asymmetric, with a steep slope at high energies and a long tail at low energies. Also, both have a maximum at 2.9 eV. These features reflect the shape of the density of states of the lower plasmon branch shown in Fig. 3. The plasmon spontaneous emission enhancement $F_p\approx 49$ in the theoretical curve is 15% lower than the experimental $F_p\approx 56$, but considering that the theory has no adjustable parameters, this still is a remarkable result. In addition, the experimental spectrum ($Q\approx 15$) is broader than the calculated curve, ($Q\approx 60$). This might be attributed to Ag film roughness or damping of the electron motion in the Ag. The Purcell enhancement factor $F_p\approx 56$, is controlled by the available area in the two-dimensional surface-plasmon dispersion k space. The k cutoff is determined by the 12-nm spacing between the quantum well and the Ag film, which weakens the fringing electric field of high wave-vector modes. A narrower spacing would have produced a correspondingly larger value of F_p.

The photophysics of a semiconductor radiator is inherently different from the photophysics of a molecule above a silver surface. Classic experiments, similar to those reported here,[1,6] were performed by Drexhage for molecules spaced above a silver surface. Those results were interpreted[2] in terms of the two radiative mechanisms, external emission, and surface-plasmon emission. In addition, a third de-excitation channel[2] was invoked, ''lossy surface waves,'' that really consists of electron-hole intraband excitations in the Ag Fermi sea. Momentum matching to electrons in the Fermi sea requires large wave-vector electromagnetic fields, as associated with a molecular point dipole radiator. Since semiconductor wave functions are spatially extended, the corresponding electric dipole fluctuations have a long wavelength and intraband excitation in the Ag Fermi sea will be momentum disallowed. Thus, the SQW can be safely spaced even closer than the 12 nm used in these experiments, allowing a larger wave vector cutoff, and a correspondingly larger plasmon Purcell effect proportional to the inverse square of that spacing. Therefore, a semiconductor quantum well near Ag eliminates nonradiative intraband dissipation in the metal that was present for closely spaced molecular radiators. The allowed closer spacing of semiconductors can permit a Purcell factor >1000, without incurring dissipation due to ''lossy surface waves,'' or intraband excitations, contrary to the case of molecular radiators.

In summary, we have demonstrated a direct coupling of electron and holes in a 3-nm InGaN/GaN SQW to the surface plasmons of an 8-nm silver layer spaced 12 nm away from the quantum well. The relevant plasmon modes correspond to the tangential (symmetric) surface modes, consisting simply of ac currents flowing in the Ag film. The Purcell enhancement factor into plasmon modes competed well with external spontaneous emission, quantitatively explaining the magnitude of the spectral dip in the external light emission.

If efficient antenna nanostructures can be incorporated in the thin Ag film, it should be possible to out-couple the SP energy into the air. The result would be >50 times faster light-emitting diode modulation efficiency, a spontaneous emission that could be more readily extracted from the semiconductor, and that would compete more effectively with nonradiative processes.

[1] K. H. Drexhage, in *Progress in Optics*, edited by E. Wolf (North-Holland, Amsterdam, 1974), Vol. 12, p. 163.

[2] G. W. Ford and W. H. Weber, Phys. Rep. **113**, 195 (1984). See also R. R. Chance, A. Prock, and R. Silbey, Adv. Chem. Phys. **37**, 1 (1978).

[3] H. F. Ghaemi, Tineke Thio, D. E. Grupp, T. W. Ebbesen, and H. J. Lezec, Phys. Rev. B **58**, 6779 (1998).

[4] H. R. Stuart and D. G. Hall, Appl. Phys. Lett. **69**, 2327 (1996).

[5] N. E. Hecker, R. A. Höpfel, and N. Sawaki, Physica E **2**, 98 (1998).

[6] P. T. Worthing, R. M. Amos, and W. L. Barnes, Phys. Rev. A **59**, 865 (1999).

[7] H. Ehrenreich and H. R. Philipp, Phys. Rev. **128**, 1622 (1962).

[8] A. Liebsch, Phys. Rev. Lett. **71**, 145 (1993).

[9] S. Keller, S. F. Chichibu, M. Minski, E. Hu, U. K. Mishra, and S. DenBaars, J. Cryst. Growth **195**, 258 (1998).

[10] Pochi Yeh, *Optical Waves in Layered Media* (Wiley, New York, 1988), Chap. 4.

[11] A. J. McAlister and E. A. Stern, Phys. Rev. **132**, 1599 (1963).

[12] *American Institute of Physics Handbook*, 3rd ed. (McGraw-Hill, New York, 1972), pp. 6–149.

[13] D. Brunner, H. Angerer, E. Bustarret, F. Freudenberg, R. Hopler, R. Dimitrov, O. Ambacher, and M. Stutzmann, J. Appl. Phys. **82**, 5090 (1997).

[14] L. Landau and E. Lifshitz, *Electrodynamics of Continuum Media* (Pergamon, New York, 1984), p. 253.

[15] P. Milonni, *The Quantum Vacuum: an Introduction to Quantum Electrodynamics* (Academic, Boston, 1994).

[16] J. M. Gérard, B. Sermage, B. Gayral, B. Legrand, E. Costard, and V. Thierry Mieg, Phys. Rev. Lett. **81**, 1110 (1998).